Observation of the complex propagation of a femtosecond laser pulse in a dispersive transparent bulk material

Hiroshi Kumagai, Sung-Hak Cho, Kenichi Ishikawa, and Katsumi Midorikawa

Laser Technology Laboratory, RIKEN, 2-1 Hirosawa, Wako, Saitama 351-0198, Japan

Masatoshi Fujimoto, Shin-ichiro Aoshima, and Yutaka Tsuchiya

Central Research Laboratory, Hamamatsu Photonics K. K., 5000 Hirakuchi, Hamakita, Shizuoka 434-8601, Japan

Received August 15, 2002

Pulse shapes in a dispersive transparent material modulated by group-velocity dispersion, self-phase modulation, and self-focusing induced by a femtosecond laser light were observed directly with femtosecond time-resolved optical polarigraphy probing the induced instantaneous birefringence. The first observation of the state of femtosecond laser pulses about the interaction region inside the transparent bulk material indicated that the pulse propagation was accomplished with a multiple conelike structure that was hypothesized from a numerical simulation with an extended nonlinear Schrödinger equation. © 2003 Optical Society of America

OCIS codes: 320.2250, 260.1440, 320.7100, 350.5500, 140.3440.

1. INTRODUCTION

Since the advent of intense femtosecond lasers, the propagation behavior of femtosecond pulses has attracted considerable attention[1] because various self-modulating linear and nonlinear effects in the propagation of an intense femtosecond pulse in a medium must be interwoven with one another. The effects include the normal and high-order group velocity dispersion, transverse diffraction, self-focusing, self-steepening, self-phase modulation, self-defocusing owing to plasma formation, and multiphoton absorption.

Over the past decade the propagation of intense femtosecond pulses in gaseous media has been investigated intensively.[2–5] Localization of the intensity of the pulse was reported as the formation of the optical filamentation and splitting of the pulse along the propagation axis. For observation of this phenomenon, the long-lived gradient in the refractive index was examined as indirect diagnostics by the schlieren method.[6] Some authors demonstrated a direct method of femtosecond time-resolved optical polarigraphy (FTOP) for observing pulse propagation of a focused femtosecond laser in air.[7] This method uses the instantaneous birefringence induced by the large electrical field of the pulse. Through consecutive femtosecond snapshot images of intense femtosecond laser pulses propagating in air, ultrafast temporal changes in the two-dimensional spatial distribution of the optical pulse intensity were clearly observed.

Recently, bulk modifications of various transparent materials, e.g., quartz glass, by use of intense femtosecond laser pulses have attracted much interest[8–12] because the laser pulse facilitates easy multiphoton absorption of the transparent materials with wide bandgaps.[13] These materials are more dispersive than gaseous media, resulting in the more complex propagation of the intense femtosecond laser pulse, assuming plasma formation through multiphoton ionization and avalanche ionization. Inside the bulk, where an intense femtosecond laser pulse is focused, there appear (i) coloration of the transparent material through the laser-induced formation of color centers and the laser-induced oxidation-reduction reaction of active ions of rare-earth elements, transition metals, and heavy metals, (ii) high-density defects, resulting in a change in refractive index,[8] (iii) voids formed by laser-driven microexplosions,[14] and (iv) microcracks caused by optical breakdown. These structures are attractive for three-dimensional optical memory,[9,12] waveguides,[15] and photonic crystals[16] because of the selective spatial distribution of the refractive index. Nevertheless, no direct diagnostic technique has been developed for observing the instantaneous intensity distribution of the self-modulating pulse as it propagates in bulk. Indeed, precise inside-bulk machining will be achieved when we understand precisely the phenomena of the interactions between the intense femtosecond laser pulse and the transparent material. Then we can control the wave packet of the pulse to make it suitable for inside-bulk machining by observation of the instantaneous wave packet.

2. EXPERIMENTAL METHOD

We introduce a general scheme for FTOP in a transparent bulk material. As shown in Fig. 1, the intense light pulse to be measured, called the pump pulse, propagates along the z axis in an isotropic medium. The pump pulse is linearly polarized, with its electric field in the x direction. A probe pulse is introduced and then propagates along the y axis. The probe pulse is sufficiently weak and has a lin-

0740-3224/2003/030597-06$15.00

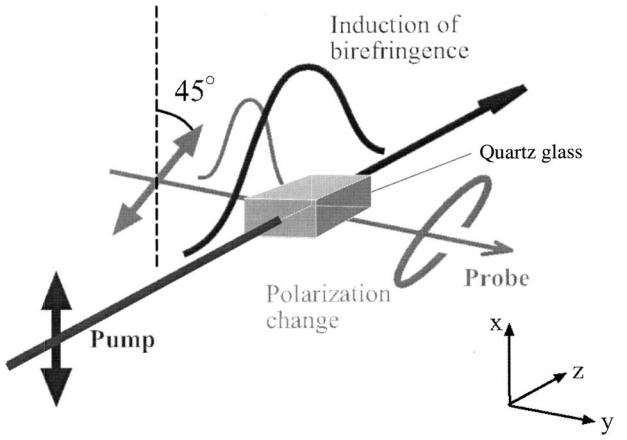

Fig. 1. The pump–probe arrangement of FTOP. The single-headed arrows indicate the propagation directions of the pulses. Both pulses are linearly polarized, and the directions of the vibrations of their electric fields are indicated by the double-headed arrows. The anisotropic change of refractive index in quartz glass is induced by the pump pulse according to its intensity distribution. The probe pulse senses the birefringence, and its polarization state is altered. The amount of probe-polarization change reflects the instantaneous intensity distribution of the pump pulse.

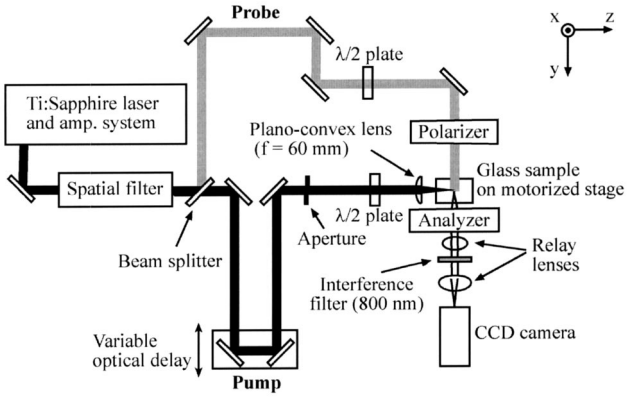

Fig. 2. Schematic of the FTOP. The beam from the laser system is split into a pump and a probe. The pump, with an electric field redirected along the x axis, is focused in the quartz glass. The probe is synchronously irradiated into the glass and experiences an induced refractive-index change caused by the large electric field of the pump. For effective extraction of the pump-intensity information, the direction of the vibration of the probe's electric field component perpendicular to the incident field is extracted by the analyzer after interaction with the pump-induced birefringence. The extracted probe component is detected by the CCD camera with a relay lens to produce images of the instantaneous intensity distribution of the pump.

ear polarization of angle θ, which represents the direction of its electric field from the x axis in the xz plane. Each frequency component is represented by one and the same frequency value, and this condition can be achieved when the frequency width is sufficiently narrow that it does not change the way in which the medium responds. This approximation is appropriate for a response that originates from electronic motion without resonance, provided that the widths of the pulses employed are more than several tens of femtoseconds. Figure 2 is a schematic of the experimental setup for FTOP in a quartz glass. Intense optical pulses (130 fs, 9 mJ, 10 Hz, 800 nm) of linear polarization with an electric field in the horizontal plane from a Ti:sapphire amplifier system are split into a pump and a probe. After the pump beam passes through the variable optical delay, the direction of vibration of the electric field is changed to vertical by a half-wave plate; then the beam is focused into a quartz glass by a plano–convex focusing lens (f = 60 mm at 632 nm). The diameter and the energy of the pump beam are reduced from 13 to 3.2 mm and from ~8 to ~1.4 mJ, respectively. The quartz glass moves slowly during the measurement, so damage does not accumulate at a certain position. Meanwhile, the collimated probe pulse synchronously irradiates the area about the focal point. By the use of the polarizer after the half-wave plate, the linear polarization angle of the probe is set to exactly 45° with respect to the horizontal plane of the optical bench. After the pulse passes through the interaction region, only the components that are perpendicular to the polarizer are extracted by the analyzer. The relay lenses magnify the image, which is then detected by a CCD camera with a 2.26-μm/pixel scale, corresponding to a 7.5-fs/pixel scale in vacuum. The energy of the pump pulse is controlled by insertion of suitable neutral-density filters into the pump path.

3. EXPERIMENTAL RESULTS

Figure 3 shows some of the time-resolved images of 14.8-μJ [Fig. 3(A)] and 135-μJ [Fig. 3(B)] pump pulse propagations in quartz glass. The pump pulse propagates from top to bottom in each image, and time proceeds from left to right. The numbers at the bottom represent the time delay from image (a). Each image is integrated 10 times, and the background is subtracted. Figure 3(A)

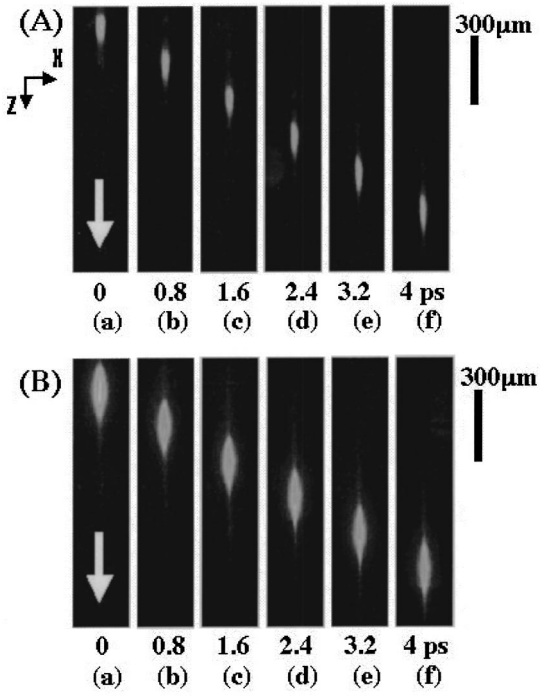

Fig. 3. FTOP images of (A) 14.8-μJ and (B) 135-μJ pump pulses propagating in a quartz glass. The optical pump pulse, which is the object of the image, propagates from top to bottom.

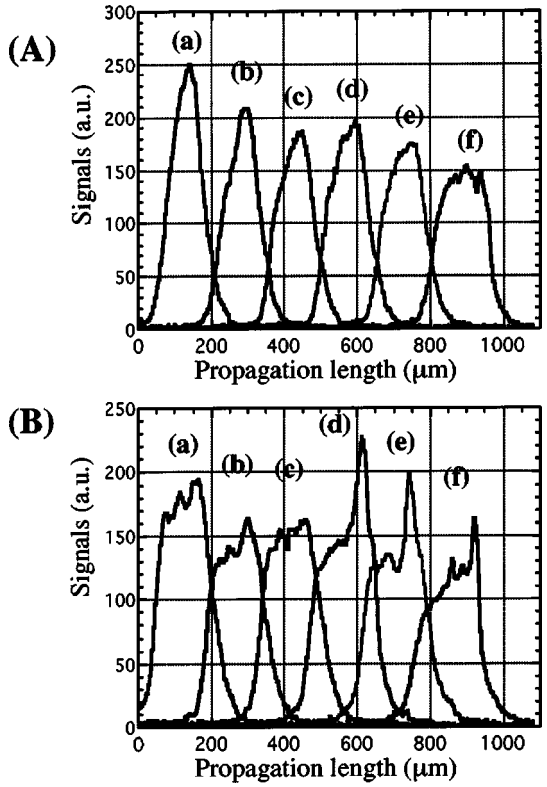

Fig. 4. Profiles of (A) 14.8-μJ and (B) 135-μJ pump pulse propagations in quartz glass along the propagation axes of the FTOP images shown in Figs. 3(A) and 3(B), respectively. Time delays of (b), (c), (d), (e), and (f) from (a) are 0.8, 1.6, 2.4, 3.2, and 4.0 ps, respectively.

shows pulse durations 326, 416, 341, 403, 497, 536, and 574 fs. Figure 3(B) shows some of the time-resolved images of 135-μJ pump pulse propagation in a quartz glass. The pulse durations of images (a), (b), and (c) are 1.12, 1.17, and 1.23 ps, respectively, which are longer than those of the 14.8-μJ pump pulse by approximately a factor of 3 and are also longer than those of the initial pump pulse by approximately a factor of 10. This pulse broadening is due to the combination of self-phase modulation induced by the intense femtosecond laser and group-velocity dispersion. Particularly for the pump energy of 135 μJ, FTOP of self-focusing is clearly observed about the focal point.

Figure 4 shows the profiles of the FTOP images of Fig. 3 along the propagation axis. Profile (a) in Fig. 4(A) is an ideal profile, like that of an optimal Gaussian pulse, whereas the pulse peaks in profiles (b)–(e) are found to shift toward the trailing edge as a result of the self-steepening effect induced by the intensity dependence of the group velocity.

All profiles in Fig. 4(B) have remarkable structures at the top, particularly profile (d), which indicates a sharp peak at the leading edge. The sharp peak at the leading edge in FTOP should be evidence of pulse propagation with a multiple conelike structure, as we discuss below with a numerical simulation.

4. NUMERICAL SIMULATION

To understand these complicated results better, we numerically simulated the propagation of intense femtosecond laser pulses inside quartz glass. Figure 5 shows a schematic of laser propagation for the numerical simulation. The spacing between the input end of the quartz glass and the linear focal point is 7.5 mm. The shape of the pulse before it is injected into the glass is assumed to be that of a hyperbolic-secant pulse in time and a Gaussian profile in lateral space. The beam radius at the input end is 200 μm. Assuming propagation along the z axis, we model the evolution of the complex envelope $E(r, z, t)$ of the electric field $\varepsilon(r, z, t) = E(r, z, t)\exp(ik_0 z - i\omega_0 t)$ with the following extended nonlinear Schrödinger equation[17–20] in a reference frame moving at the group velocity:

$$\frac{\partial E}{\partial z} + \frac{i}{2}\beta_2\frac{\partial^2 E}{\partial t^2} - \frac{1}{6}\beta_3\frac{\partial^3 E}{\partial t^3} - \frac{i}{2n_0k_0}\left(\frac{\partial^2}{\partial r^2} + \frac{1}{r}\frac{\partial}{\partial r}\right) \times \left(1 - \frac{i}{\omega_0}\frac{\partial}{\partial t}\right)E = in_2k_0\left(1 + \frac{i}{\omega_0}\frac{\partial}{\partial t}\right)(|E^2|E) - \frac{ik_0}{2}\left(1 - \frac{i}{\omega_0}\frac{\partial}{\partial t}\right) \times \left(\frac{\rho}{\rho_{cr}}E\right) - 3\sigma_6(\rho_0 - \rho)\left(\frac{|E^2|}{\hbar\omega_0}\right)^5 E. \quad (1)$$

E is normalized in such a way that $|E|^2$ gives an intensity in watts per square centimeter for convenience. The second through the fourth terms on the left-hand side of Eq. (1) describe the second-order and the third-order group-velocity dispersion and the transverse diffraction, respectively. The terms on the right-hand side describe the nonlinear Kerr response of a quartz glass, plasma defocusing, and multiphoton absorption. We have also included self-steepening, space–time focusing, and the correction compensating for the plasma defocusing to account for the correction beyond the slowly varying envelope approximation caused by the shortness of the pulse.

We choose a laser operating wavelength of $\lambda_0 = 800$ nm, which corresponds to angular frequency $\omega_0 = 2.35\ \mathrm{fs}^{-1}$ and vacuum wave number $k_0 = 7.85\ \mu\mathrm{m}^{-1}$. The material parameters used in our simulations for quartz glass are as follows: $\beta_1 = 4.894\ \mu\mathrm{m}^{-1}\,\mathrm{fs}$, β_2

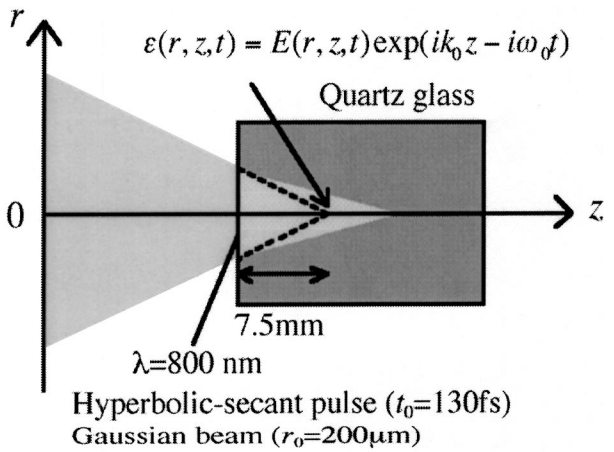

Fig. 5. Schematic of laser propagation for the numerical simulation.

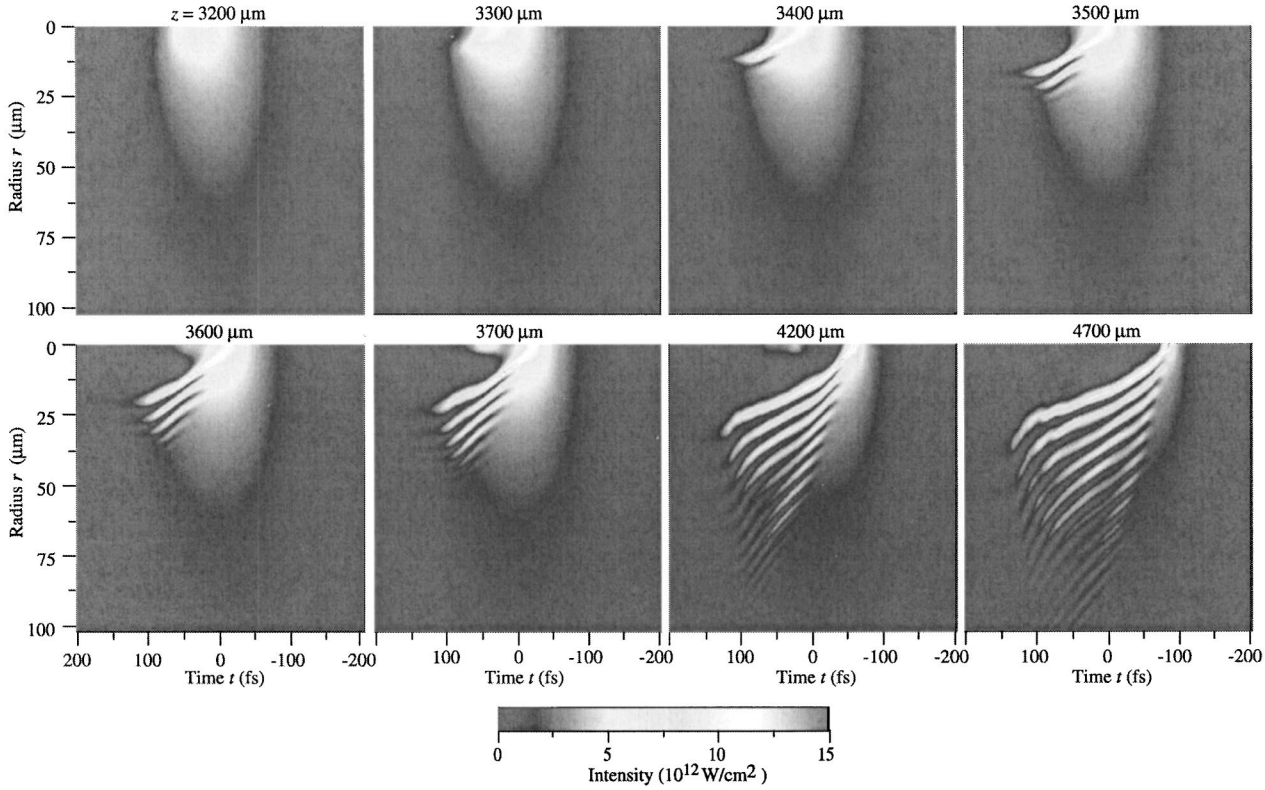

Fig. 6. Simulated spatiotemporal profiles of the laser intensity at several propagation distances z for an input energy of 135 μJ.

$= 0.034\ \mu\text{m}^{-1}\,\text{fs}^2$, $n_0 = 1.4533$, and $n_2 = 2.66 \times 10^{-16}\,\text{cm}^2/\text{W}$. Critical electron density ρ_{cr} for $\lambda_0 = 800$ nm is $1.74 \times 10^{21}\ \text{cm}^{-3}$, and the initial electron density ρ_0 in the valence band is $2.23 \times 10^{22}\ \text{cm}^{-3}$. ρ is the density of electrons produced through six-photon band-to-band transitions, as the bandgap is 9.0 eV. Cross section σ_6 for the process is evaluated from Keldysh theory to be $2.6 \times 10^{-180}\ \text{s}^5\,\text{cm}^{12}$.[21] Equation (1) is combined with an equation for the density of electrons produced through multiphoton band-to-band transitions:

$$\frac{\partial \rho}{\partial t} = \sigma_6 \left(\frac{|E|^2}{\hbar \omega_0} \right)^6 (\rho_0 - \rho). \tag{2}$$

The numerical scheme for solving Eq. (1) is based on the split-step Fourier method.[22] The diffraction term is treated by the Peaceman–Rachford method.[23] The nonlinear terms as well as Eq. (2) are integrated by the Runge-Kutta method. We verified the numerical results by doubling the space and time resolution, which led to no significant change in the behavior of the results presented here.

Figure 6 illustrates the spatiotemporal laser intensity profile at several propagation distances z for the input energy of 135 μJ obtained under the initial boundary conditions that are similar to those in the experiments. By $z = 3200\ \mu$m, the pulse energy is concentrated near the beam axis as a result of the self-focusing effect induced by the intensity-dependent refractive index, and the pulse peak is shifted toward the trailing edge because of the self-steepening effect induced by the intensity dependence of the group velocity. As the self-focusing proceeds and the local intensity increases further, free (plasma) electrons are produced through multiphoton absorption. Because the plasma formation has a negative effect on the refractive index, defocusing occurs near the trailing edge ($z = 3300\ \mu$m) and results in the formation of a conelike structure ($z = 3400\ \mu$m). At $z = 3400\ \mu$m, we can see that a second cone begins to be formed outside the first cone. With pulse propagation, more and more cones are formed, resulting in the formation of a multiple conelike structure at $z = 4200\ \mu$m. It can also be seen that the pulse is temporally split near the axis.

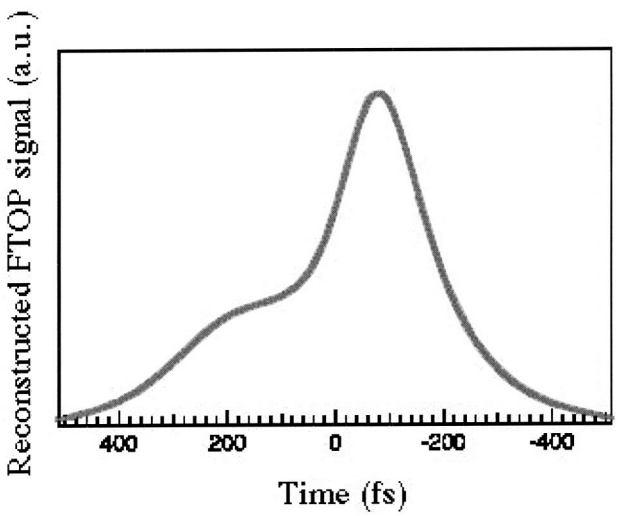

Fig. 7. Reconstructed FTOP signal at 4200 μm.

We may define a self-trapping power P_{cr} ($P_{\text{cr}} = \lambda_0^2/2\pi n_0 n_2$) as the power for which the wave-front cur-

vature that is due to diffraction is exactly compensated for by the wave-front curvature that is due to self-focusing, where λ_0 denotes the laser wavelength, n_0 is the linear refractive index, and n_2 is the nonlinear refractive index. At a power P smaller than P_{cr}, the pulse propagation is essentially linear. When the power is slightly higher than P_{cr} (as much as several times P_{cr}), various phenomena such as filamentation and pulse splitting appear. In the present case, the self-trapping power for quartz glass is a power of 2.2×10^6 W, whereas a pulse with a duration of 130 fs and an energy of 135 μJ translates into a power of 10^9 W. In such a case the self-focusing effect is so dramatic that a local intensity maximum can absorb a large amount of energy from its direct vicinity and form another local intensity maximum outside it. Repetition of this procedure leads to the multiple conelike structure shown in Fig. 6. We can see more than 14 cones in the pulse. Thus the multiple conelike structure is a new feature that emerges only when the pulse power is orders of magnitude higher than P_{cr}. In this regime the evolution of the spatiotemporal beam profile is dominated largely by the nonlinear Kerr response and plasma defocusing. Self-steepening and space–time focusing, which play important roles when the pulse power is slightly higher than P_{cr}, have only small effects on the profile. It is also striking that the multiple cone formation is completed during a short interval of several hundreds of micrometers and that this structure propagates stably over 1 mm.

Now that we have a spatiotemporal intensity profile at each propagation distance, we can calculate a FTOP signal, which is expected to be observed. We show this calculated FTOP signal at $z = 4200$ μm in Fig. 7. In this figure the main features observed in experimentally obtained FTOP signals (Fig. 4), such as a peak near the leading edge and a shoulder near the trailing edge, are reproduced very well. These reproduced features suggest pulse propagation with a multiple conelike structure. As discussed in Ref. 24, the captured images in FTOP experiments mean instantaneous intensity distribution of the pump pulse. However, we note that the experimental data are integrated unavoidably along the y direction. Therefore the effect of the projection onto the plane parallel to the detector, although it is common for each case for image detection, makes it difficult to observe the pulse propagation with a multiple conelike fine structure seen in the theoretical plot, whereas we would rather find the integrated image of the pulse propagation along the y direction with a resolution of ~18 fs, which is limited by the numerical aperture of the imaging lens used in this study. If the incident angle of the probe pulse to the pump pulse is variable, we might obtain evidence of pulse propagation with a multiple conelike fine structure from a comparison of experiments with different angles of the probe pulse.

5. CONCLUSIONS

In conclusion, modulated pulse shapes in a quartz glass were observed directly with femtosecond time-resolved optical polarigraphy probing the induced instantaneous birefringence. The first observation of the state of a femtosecond laser pulse about the interaction region inside the transparent bulk material indicated complicated propagation of the pulse, with a sharp peak at the leading edge owing to the combination of normal and high-order group-velocity dispersion, transverse diffraction, self-focusing, self-steepening, self-phase modulation, and self-defocusing that results from multiphoton ionization and plasma formation.

The FTOP image of the pulse was also reproduced well by a numerical simulation with an extended nonlinear Schrödinger equation, such as a peak near the leading edge and a shoulder near the trailing edge. The numerical simulation also suggested pulse propagation with a multiple conelike structure.

ACKNOWLEDGMENTS

This study is supported partially by special coordination funds for promoting science and technology from the Ministry of Education, Culture, Sports, Science and Technology of the Japanese government.

H. Kumagai's e-mail address is hkumagai @postman.riken.go.jp

REFERENCES

1. A. Braun, G. Kohn, X. Liu, D. Du, J. Squier, and G. Mourou, "Self-channeling of high-peak-power femtosecond laser pulses in air," Opt. Lett. **20**, 73–75 (1995).
2. A. B. Borisov, A. V. Borovskiy, V. V. Korobkin, A. M. Prokhorov, O. B. Shiryaev, X. M. Shi, T. S. Luk, A. McPherson, J. C. Solem, K. Boyer, and C. K. Rhodes, "Relativistic and charge-displacement self-channeling of intense subpicosecond ultraviolet (248 nm) radiation in plasmas," Phys. Rev. Lett. **68**, 2309–2312 (1992).
3. A. Pukhov and J. Meyer-ter-Vehn, "Relativistic magnetic self-channeling of light in near-critical plasma: three-dimensional particle-in-cell simulation," Phys. Rev. Lett. **76**, 3975–3978 (1996).
4. J. Fuchs, G. Malka, J. C. Adam, F. Amiranoff, S. D. Baton, N. Blanchot, A. Héron, G. Laval, J. L. Miquel, P. Mora, H. Pépin, and C. Rousseaux, "Dynamics of subpicosecond relativistic laser pulse self-channeling in an underdense preformed plasma," Phys. Rev. Lett. **80**, 1658–1661 (1998).
5. M. Borghesi, A. J. Mackinnon, R. Gaillard, O. Willi, A. Pukhov, and J. Meyer-ter-Vehn, "Large quasistatic magnetic fields generated by a relativistically intense laser pulse propagating in a preionized plasma," Phys. Rev. Lett. **80**, 5137–5140 (1998).
6. C. E. Clayton, K. C. Tzeng, D. Gordon, P. Muggli, W. B. Mori, C. Joshi, V. Malka, Z. Najmundin, A. Modena, D. Neely, and A. E. Dangor, "Plasma wave generation in a self-focused channel of a relativistically intense laser pulse," Phys. Rev. Lett. **81**, 100–103 (1998).
7. M. Fujimoto, S. Aoshima, M. Hosoda, and Y. Tsuchiya, "Femtosecond time-resolved optical polarigraphy: imaging of the propagation dynamics of intense light in a medium," Opt. Lett. **24**, 850–852 (1999).
8. K. M. Davis, K. Miura, N. Sugimoto, and K. Hirao, "Writing waveguides in glass with a femtosecond laser," Opt. Lett. **21**, 1729–1731 (1996).
9. E. N. Glenzer, M. Milosavljevic, L. Huang, R. J. Finlay, T. H. Her, J. P. Callan, and E. Mazur, "Three-dimensional optical storage inside transparent materials," Opt. Lett. **21**, 2023–2025 (1996).
10. D. Ashkenasi, H. Varel, A. Rosenfeld, S. Henz, J. Herrmann, and E. E. B. Cambell, "Application of self-focusing of ps laser pulses for three-dimensional microstructuring of

transparent materials," Appl. Phys. Lett. **72**, 1442–1444 (1998).
11. S.-H. Cho, H. Kumagai, I. Yokota, K. Midorikawa, and M. Obara, "Observation of self-channeling plasma formation and bulk modification in optical fibers using high-intensity femtosecond laser," Jpn. J. Appl. Phys. **37**, L737–L739 (1998).
12. M. Watanabe, H.-B. Sun, S. Juodkazis, T. Takahashi, S. Matsuo, Y. Suzuki, J. Nishi, and H. Misawa, "Three-dimensional optical data storage in vitreous silica," Jpn. J. Appl. Phys. **37**, L1527–L1530 (1998).
13. D. Du, X. Liu, G. Korn, J. Squier, and G. Mourou, "Laser-induced breakdown by impact ionization in SiO_2 with pulse widths from 7 ns to 150 fs," Appl. Phys. Lett. **64**, 3071–3073 (1994).
14. E. N. Glenzer and E. Mazur, "Ultrafast-laser driven micro-explosions in transparent materials," Appl. Phys. Lett. **71**, 882–884 (1997).
15. K. Miura, J. Qiu, H. Inouye, T. Mitsuyu, and K. Hirao, "Photowritten optical waveguides in various glasses with ultrashort pulse laser," Appl. Phys. Lett. **71**, 3329–3331 (1997).
16. H.-B. Sun, Y. Xu, S. Juodkazis, K. Sun, M. Watanabe, S. Matsuo, H. Misawa, and J. Nishii, "Arbitrary-lattice photonic crystals created by multiphoton microfabrication," Opt. Lett. **26**, 325–327 (2001).
17. J. E. Rothenberg, "Space–time focusing: breakdown of the slowly varying envelope approximation in the self-focusing of femtosecond pulses," Opt. Lett. **17**, 1340–1342 (1992).
18. J. K. Ranka and A. L. Gaeta, "Breakdown of the slowly varying envelope approximation in the self-focusing of ultrashort pulses," Opt. Lett. **23**, 534–536 (1998).
19. L. Bergé and A. Couairon, "Gas-induced solitons," Phys. Rev. Lett. **86**, 1003–1006 (2001).
20. N. Aközbek, M. Scalora, C. M. Bowden, and S. L. Chin, "White-light continuum generation and filamentation during the propagation of ultra-short laser pulses in air," Opt. Commun. **191**, 353–362 (2001).
21. L. V. Keldysh, "Ionization in the field of a strong electromagnetic wave," Sov. Phys. JETP **20**, 1307–1314 (1965).
22. G. P. Agrawal, *Nonlinear Fiber Optics*, 2nd ed. (Academic, San Diego, Calif., 1995).
23. S. E. Koonin, K. T. R. Davies, V. Maruhn-Rezwani, H. Feldmeier, S. J. Krieger, and J. W. Negele, "Time-dependent Hartree–Fock calculations for $^{16}O + {}^{16}O$ and $^{40}Ca + {}^{40}Ca$ reactions," Phys. Rev. C **15**, 1359–1374 (1977).
24. M. Fujimoto, S. Aoshima, M. Hosoda, and Y. Tsuchiya, "Analysis of instantaneous profiles of intense femtosecond optical pulses propagating in helium gas measured by using femtosecond time-resolved optical polarigraphy," Phys. Rev. A **64**, 033813/1-11 (2001).